FULL TITLE
ASP Conference Series, Vol. **VOLUME**, **YEAR OF PUBLICATION**
NAMES OF EDITORS

Clustering, host galaxies, and evolution of AGN

Ryan C. Hickox and the Boötes survey collaboration

Harvard-Smithsonian Center for Astrophysics, 60 Garden Street, Cambridge, MA 02138

Abstract. We explore the connection between different classes of active galactic nuclei (AGNs) and the evolution of their host galaxies, by deriving host galaxy properties, clustering, and Eddington ratios of AGNs selected in the radio, X-ray, and infrared (IR) wavebands from the wide-field (9 deg^2) Boötes survey. We study a sample of 585 AGNs at $0.25 < z < 0.8$ using redshifts from the AGN and Galaxy Evolution Survey (AGES). We find that radio and X-ray AGNs reside in relatively large dark matter halos ($M_{\rm halo} \sim 3 \times 10^{13}$ and 10^{13} h^{-1} $M_\odot$, respectively) and are found in galaxies with red and "green" colors. In contrast, IR AGNs are in less luminous galaxies, have higher Eddington ratios, and reside in halos with $M_{\rm halo} < 10^{12}$ $M_\odot$. We interpret these results in terms of a general picture for AGNs and galaxy evolution, in which quasar activity is triggered when $M_{\rm halo} \sim 10^{12}$–$10^{13}$ $M_\odot$, after which star formation ceases and AGN accretion shifts to optically-faint, X-ray and radio-bright modes.

1. Introduction

It is increasingly clear that a role in galaxy evolution is played by active galactic nuclei (AGNs), as suggested by the tight correlation between supermassive black hole (SMBH) mass and galaxy bulge properties (e.g., Magorrian et al. 1998; Ferrarese & Merritt 2000; Gebhardt et al. 2000), and the ability of AGN feedback to regulate star formation in galaxy formation models (e.g., Bower et al. 2006; Hopkins et al. 2006; Croton et al. 2006; Khalatyan et al. 2008; Bower et al. 2008). Different modes of accretion may play varying roles in galaxy evolution (e.g., Merloni & Heinz 2008; Kauffmann & Heckman 2008), and observational clues to the links between AGN and galaxies come from the host properties and dark matter halo masses of different classes of AGNs. In general, low-level accretion is relatively bright in the radio and X-rays, while AGNs with higher accretion rates are readily detected in the optical and IR. Radio-selected AGNs are generally found in luminous red-sequence galaxies in massive dark matter halos (e.g., Mandelbaum et al. 2008), while X-ray AGNs reside in galaxies with "green" colors and somewhat less massive halos (e.g., Silverman et al. 2008; Gilli et al. 2008). Optical quasars are found in halos of mass $\sim 3 \times 10^{12}$ $M_\odot$ at all redshifts (e.g., Croom et al. 2005; Shen et al. 2007). These results indicate that the different modes of accretion occur at different phases in galaxy evolution. Here we present a study of the host galaxies, clustering, and Eddington ratios for three classes of AGNs (radio, X-ray, and IR-selected) in the 9 deg^2 Boötes field, and compare our results to a simple picture of AGN and galaxy evolution. We use a cosmology with $\Omega_{\rm m} = 0.3$, $\Omega_\Lambda = 0.7$, $h = 0.7$, and $\sigma_8 = 0.9$; the observations and results are described in detail in Hickox et al. (2009).

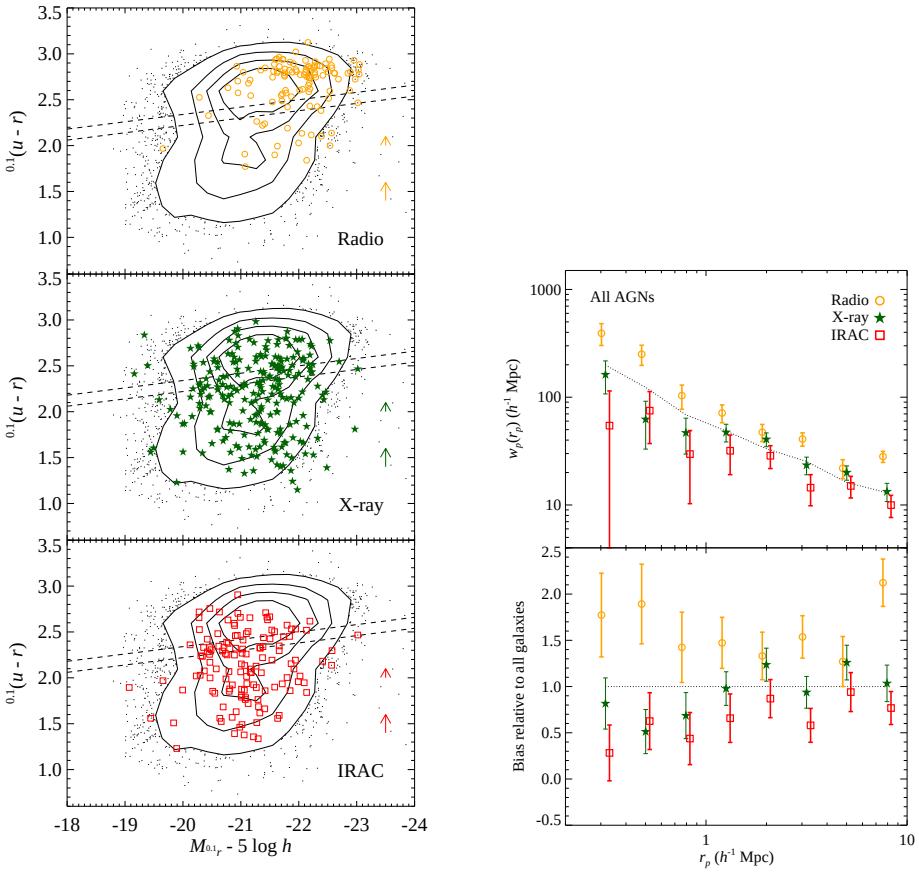

Figure 1. *Left:* Optical colors and absolute magnitudes of AGNs with extended optical counterparts. Contours and black points show the distribution for AGES galaxies, and dashed lines separate the blue cloud from the red sequence. Orange circles, green stars, and red squares show radio, X-ray, and IR AGNs, respectively. Arrows show typical (small) corrections for nuclear contamination. *Right:* The top panel shows the projected two-point cross-correlations of AGNs with respect to all AGES galaxies (symbols as at left). For comparison, the dotted lines show the autocorrelation of AGES galaxies. The bottom panel shows bias for AGNs relative to AGES galaxies.

2. Observations and AGN sample

We use data from the 9 deg^2 Boötes multiwavelength survey, with optical photometry from the NOAO Deep Wide-Field Survey (Jannuzi & Dey 1999), X-ray data from the *Chandra* XBoötes survey (Murray et al. 2005), *Spitzer* IRAC data from the IRAC Shallow Survey (Eisenhardt et al. 2004), radio data from the Westerbork Radio Telescope 1.4 GHz radio survey (de Vries et al. 2002), and redshifts from MMT/AGES (C. Kochanek et al. 2009, in preparation). We select 6262 galaxies and 585 AGNs in the redshift interval $0.25 < z < 0.8$. We select 122 radio AGNs with $P_{1.4\,\mathrm{GHz}} > 6 \times 10^{23}$ W Hz^{-1}, 362 X-ray AGNs

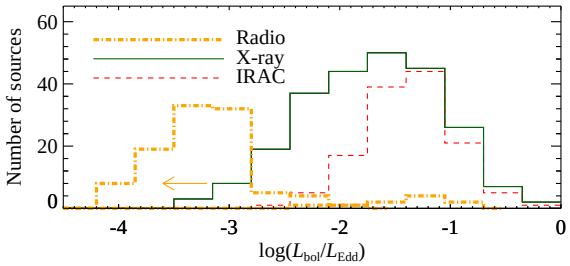

Figure 2. Distributions in Eddington ratios for AGNs with extended optical counterparts. The $L_{\rm bol}$ and $L_{\rm bol}/L_{\rm Edd}$ estimates for the X-ray undetected radio AGNs show only upper limits derived from X-ray stacking. Radio, X-ray, and IR AGNs have progressively higher typical Eddington ratios.

with $L_X > 10^{42}$ ergs s^{-1}, and 238 IR AGNs using the color-color criterion of Stern et al. (2005). Only 19 of the radio AGNs are selected in either X-rays or the IR, although there is $\approx$ 30–50% overlap between the X-ray and IR samples (for details on this overlap sample see Hickox et al. 2009).

3. AGN host galaxies, clustering, and Eddington ratios

We first derive host galaxy colors and luminosities (Fig. 1, *left*) for AGNs with extended optical counterparts (for which the nucleus is optically faint or obscured). We include a small color correction (< 0.2 mag) to account for residual contamination from the nucleus. We find that radio AGNs mainly reside in luminous red galaxies, while X-ray AGNs have a significant peak in the "green valley" of the color distribution, as seen in other surveys (e.g., Sánchez et al. 2004; Nandra et al. 2007). The IR AGNs have similar colors to the X-ray AGNs, but with a smaller "green" peak and with lower average luminosities.

We next derive characteristic halo masses of the different AGN types (for all AGNs, including optically-unresolved sources) by measuring the projected two-point cross-correlation function [$w_p(r_p)$] between AGNs and AGES galaxies on scales of $0.3 < r_p < 10$ h^{-1} Mpc (Fig. 1, *right*). Fitting a 3-D cross-correlation function of the form $\xi = (r/r_0)^{-\gamma}$, we obtain (r_0 [h^{-1} Mpc], γ) = ($6.3\pm0.6, 1.8\pm0.2$) for radio AGNs, ($4.7\pm0.3, 1.6\pm0.1$) for X-ray AGNs, and ($3.7\pm0.4, 1.5\pm0.1$) for IR AGNs. Using the autocorrelation of the AGES galaxies and a model of dark matter clustering (Smith et al. 2003), we then derive the absolute bias of the dark matter halos that host the AGNs, and convert the bias to $M_{\rm halo}$ (Sheth et al. 2001). We obtain $\log M_{\rm halo}(h^{-1}M_\odot) = 13.5^{+0.1}_{-0.2}$ for radio AGNs, $12.9^{+0.2}_{-0.3}$ for X-ray AGNs, and $11.7^{+0.6}_{-1.5}$ for IR AGNs.

Finally, we derive Eddington ratios ($\lambda = L_{\rm bol}/L_{\rm Edd}$) for the AGNs with extended optical counterparts (Fig. 2). We estimate $M_{\rm BH}$ from the $L_{\rm bulge}$–$M_{\rm BH}$ relation (Marconi & Hunt 2003), and derive $L_{\rm bol}$ using X-ray and IR bolometric corrections (Hopkins et al. 2007). Radio AGNs have very low Eddington ratios ($\lambda \lesssim 10^{-3}$), while X-ray AGNs have intermediate ratios ($10^{-3} \lesssim \lambda \lesssim 1$) and IR AGNs have high ratios ($\lambda \gtrsim 0.01$).

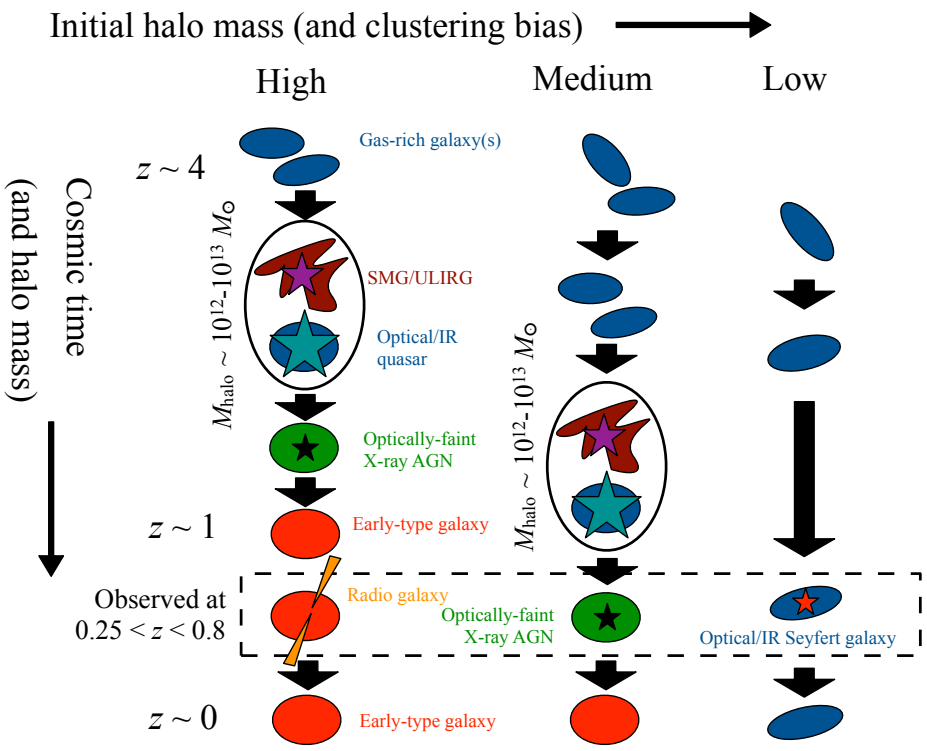

Figure 3. Simple schematic of AGN and galaxy evolution, as described in § 4. Ovals represent the quasar/starburst phase when $M_{\rm halo} \sim 10^{12}$–$10^{13}$ $M_\odot$. The dashed box shows the classes of AGNs that are observed at $0.25 < z < 0.8$.

4. Evolutionary picture

Our results are generally consistent with a simple picture of SMBH and galaxy evolution (Fig. 3), motivated by recent observational and theoretical studies. As dark matter halos increase in mass through the hierarchical growth of structure, galaxies initially form as cold gas-rich, star-forming systems with rotationally-dominated dynamics. When the dark matter halo reaches a mass $M_{\rm crit} \sim 10^{12}$–$10^{13}$ $M_\odot$ (shown by the ovals in Fig. 3), starburst and luminous AGN (quasar) activity is fueled, for example by a major galaxy merger or disk instabilities. Subsequently, star formation is quenched either by quasar feedback (Hopkins et al. 2006), or by the creation of a virialized hot halo of gas that can no longer efficiently cool (Dekel & Birnboim 2006). At later times and higher masses, lower-Eddington (X-ray and radio-bright) accretion (e.g., Churazov et al. 2005) may help prevent star formation (e.g., Bower et al. 2006; Croton et al. 2006).

In this picture, our observed population of radio AGNs represents a low-Eddington mode of accretion found in passive galaxies with high-mass halos

($M_{\rm halo} > M_{\rm crit}$). These galaxies have already experienced the quasar phase and the quenching of star formation. The observed X-ray AGNs are in a somewhat higher-Eddington phase that occurs in halos closer to $M_{\rm crit}$, during the transition of the galaxy from the blue cloud to the red sequence, while the observed IR-selected AGNs are the highest-Eddington population, found in star-forming galaxies with small black holes and dark matter halos that have not yet grown to $M_{\rm crit}$. This simple evolutionary picture naturally accounts for the observed trends in host galaxies, clustering, and Eddington ratios of the different classes of AGNs. In the future we will explore this scenario in more detail, by comparing our results with detailed predictions of galaxy formation models.

Acknowledgments. R.C.H. was supported by *Chandra* grants GO5-6130A and GO5-6121A.

References

Bower, R. G., Benson, A. J., Malbon, R., Helly, J. C., Frenk, C. S., Baugh, C. M., Cole, S., & Lacey, C. G. 2006, MNRAS, 370, 645
Bower, R. G., McCarthy, I. G., & Benson, A. J. 2008, MNRAS, 390, 1399
Churazov, E., Sazonov, S., Sunyaev, R., Forman, W., Jones, C., & Böhringer, H. 2005, MNRAS, 363, L91
Croom, S. M., et al. 2005, MNRAS, 356, 415
Croton, D. J., et al. 2006, MNRAS, 365, 11
de Vries, W. H., Morganti, R., Röttgering, H. J. A., Vermeulen, R., van Breugel, W., Rengelink, R., & Jarvis, M. J. 2002, AJ, 123, 1784
Dekel, A. & Birnboim, Y. 2006, MNRAS, 368, 2
Eisenhardt, P. R., et al. 2004, ApJS, 154, 48
Ferrarese, L. & Merritt, D. 2000, ApJ, 539, L9
Gebhardt, K., et al. 2000, ApJ, 539, L13
Gilli, R., et al. 2008, A&A in press (arXiv:0810.4769)
Hickox, R. C., et al. 2009, ApJ in press (arXiv:0901.4121)
Hopkins, P. F., Hernquist, L., Cox, T. J., Di Matteo, T., Robertson, B., & Springel, V. 2006, ApJS, 163, 1
Hopkins, P. F., Richards, G. T., & Hernquist, L. 2007, ApJ, 654, 731
Jannuzi, B. T. & Dey, A. 1999, in ASP Conf. Ser. 191: Photometric Redshifts and the Detection of High Redshift Galaxies, ed. R. Weymann, L. Storrie-Lombardi, M. Sawicki, & R. Brunner (San Francisco: ASP), 111
Kauffmann, G. & Heckman, T. M. 2008, submitted to MNRAS (arXiv:0812.1224)
Khalatyan, A., Cattaneo, A., Schramm, M., Gottlöber, S., Steinmetz, M., & Wisotzki, L. 2008, MNRAS, 387, 13
Magorrian, J., et al. 1998, AJ, 115, 2285
Mandelbaum, R., Li, C., Kauffmann, G., & White, S. D. M. 2008, submitted to MNRAS (arXiv:0806.4089)
Marconi, A. & Hunt, L. K. 2003, ApJ, 589, L21
Merloni, A. & Heinz, S. 2008, MNRAS, 388, 1011
Murray, S. S., et al. 2005, ApJS, 161, 1
Nandra, K., et al. 2007, ApJ, 660, L11
Sánchez, S. F., et al. 2004, ApJ, 614, 586
Shen, Y., et al. 2007, AJ, 133, 2222
Sheth, R. K., Mo, H. J., & Tormen, G. 2001, MNRAS, 323, 1
Silverman, J. D., et al. 2008, ApJ, 675, 1025
Smith, R. E., et al. 2003, MNRAS, 341, 1311
Stern, D., et al. 2005, ApJ, 631, 163